



Article

Controlling of Conductivity and Morphological Properties of Hole-Transport Layer Using Ionic Liquid for Vacuum-Free Planar Hybrid Solar Cells

Viet Thanh Hau Pham ¹, Thanh Kieu Trinh ², Hamid M. Shaikh ^{3,*}, Saeed M. Al-Zahrani ³, Abdullah Alhamidi ³, Sami Bin Dahman ³, Mohaseen S. Tamboli ⁴, and Nguyen Tam Nguyen Truong ^{5,*}

- Department of Chemistry and Environment, Da Lat University, Dalat 66100, Lam Dong, Vietnam
- Department of Biotechnology and Environment, Yersin University of Da Lat, Dalat 66100, Lam Dong, Vietnam
- ³ SABIC Polymer Research Center (SPRC), Department of Chemical Engineering, King Saud University, P.O. Box 800, Riyadh 11421, Saudi Arabia
- ⁴ Korea Institute of Energy Technology (KENTECH), 200 Hyeokshin-ro, Naju 58330, Republic of Korea
- School of Chemical Engineering, Yeungnam University, 280 Daehak-Ro, Gyeongsan 38541, Republic of Korea
- * Correspondence: hamshaikh@ksu.edu.sa (H.M.S.); tamnguyentn@ynu.ac.kr (N.T.N.T.)

Abstract: In this study, an acidic (A) and pH-neutral (pHN) solution using poly(3,4-ethylenedioxythiophene): poly(styrenesulfonate) (PEDOT:PSS) as the hole-transport layer (HTL) was modified using a 1-butyl-3-methylimidazolium chloride (BMIM+Cl⁻) ionic liquid (IL). The effects of this ionic liquid on the conductivity and morphological properties of the PEDOT:PSS films were investigated. The conductivity and morphological properties of the PEDOT: PSS films before and after adding IL were measured using a UV-vis spectrophotometer and atomic force microscope (AFM), respectively. The conductivity of the A-PEDOT:PSS-film-based ionic liquid was decreased, while the conductivity of the pHN-PEDOT:PSS-film-based ionic liquid was slightly decreased, while the conductivity of the pHN-PEDOT:PSS-film-based ionic liquid was slightly increased. The vacuum-free planar hybrid solar cells (VFPHSCs) using the pHN-PEDOT:PSS-film-based ionic liquid show a higher power conversion efficiency (PCE) than the VFPHSCs using the A-PEDOT:PSS-film-based ionic liquid. We also report that a solar cell with a structure of ITO/pHN-PEDOT:PSS/PTB7:PCBM/PEO/EGaIn has a maximum PCE of about ~5%.

Keywords: vacuum free; conductivity; hybrid; surface roughness; ionic liquid



Citation: Pham, V.T.H.; Trinh, T.K.; Shaikh, H.M.; Al-Zahrani, S.M.; Alhamidi, A.; Bin Dahman, S.; Tamboli, M.S.; Truong, N.T.N. Controlling of Conductivity and Morphological Properties of Hole-Transport Layer Using Ionic Liquid for Vacuum-Free Planar Hybrid Solar Cells. *Energies* 2023, 16, 467. https://doi.org/10.3390/ en16010467

Academic Editor: Philippe Leclère

Received: 25 November 2022 Revised: 22 December 2022 Accepted: 27 December 2022 Published: 1 January 2023



Copyright: © 2023 by the authors. Licensee MDPI, Basel, Switzerland. This article is an open access article distributed under the terms and conditions of the Creative Commons Attribution (CC BY) license (https://creativecommons.org/licenses/by/4.0/).

1. Introduction

The energy from photovoltaic cell (or solar cells) is the most appealing solution to solve the fossil fuel shortage problem. In comparison to their conventional inorganic counterparts, organic polymer solar cells (OSCs) have gained a lot of attention, since they have several advantages such as a low cost, solution-based processing, and the ability to fabricate devices on flexible substrates [1]. Until now, the most successful organic solar cells have been based on a hybrid architecture [2]. In a hybrid structure, the conjugated polymer donor and fullerene acceptor are mixed together, forming an interpenetrating network of nanodomains phase-separated by both a donor and an acceptor in the active thin film layer. More efficient exciton dissociation was achieved due to the large interfacial area of these interpenetrating networks, leading to higher efficiency device performance [3]. With significant efforts toward a better understanding of the basic operating mechanisms and performance optimization, a power conversion efficiency (PCE) of up to 12% for hybrid conjugated polymer-based solar cells has been reported recently [1,4].

The power conversion efficiency of polymer bulk heterojunction solar cells can be further improved by several approaches, which include developing new materials [5]; optimizing the loading amount and weight ratio of the polymer donor–fullerene acceptor [6];

Energies **2023**, 16, 467 2 of 11

controlling the morphology of the blended active layer by using thermal annealing [7–9], solvent annealing [10,11], or additives [12,13]; enhancing the electronic and electrical properties by the insertion of an proper interfacial layer between the metal cathode and active layer as an electron-transporting layer (ETL) or between the ITO anode and active layer as a hole-transporting layer (HTL) [14–16]; and so on. Among them, the engineering and optimization of the interfacial layer has proven to be a very effective approach toward enhancing the performance of hybrid solar cells devices.

PEDOT:PSS has been widely applied as a hole-transporting interfacial layer in organic solar cells due to its high transparency in the visible range, high thermal and mechanical stability, strong hole affinity, and high work function close to that of ITO. It can be dispersed in water and some organic solvents, and PEDOT:PSS films can be readily fabricated through the solution spin-coating process [17]. A thin PEDOT:PSS HTL helps reduce the roughness and alternate the work function of the ITO surface, allowing for easier transportation of the free charge carriers to the electrode. However, PEDOT:PSS is known to suffer from several reported problems including low conductivity and high acidity, which is believed to corrode the surface of indium tin oxide (ITO) electrodes [18].

Commercial PEDOT:PSS films usually have conductivity below 1 S/cm. Much research has been conducted to enhance the conductivity of PEDOT:PSS. The first method employs a high boiling-point polar organic compound, such as ethylene glycol, isopropanol, or dimethyl sulfoxide (DMSO), to dilute the PEDOT:PSS dispersion. This method can enhance the conductivity of PEDOT:PSS up to 102 S/cm and reduce the surface potential, therefore improving the adhesion properties of PEDOT:PSS toward the ITO surface [19–21]. Later, the conductivity of PEDOT:PSS films could be significantly enhanced by introducing ionic liquids, inorganic salt, or anionic surfactants into the PEDOT:PSS aqueous solution [22,23]. Especially with ionic liquids' doping, the conductivity of the PEDOT:PSS film can increase up to 2084 S/cm, which is the highest reported conductivity value of PEDOT:PSS [24]. Increasing the conductivity of the PEDOT:PSS film was attributed to the inducing ability of the ionic liquid or other additive to the phase separation between the PEDOT and PSS chains, leading to the ordering of the conductive PEDOT segments in the film, which leads to a pathway of higher conductivity [22,24].

In this work, the effects of ionic liquid on the conductivity and morphological properties of the hole-transport layer, such as acidic and pH-neutral PEDOT:PSS films, were investigated. Optical properties such as the absorption and transmittance of a HTL without and with ionic liquid were analyzed using a UV-vis machine. The morphological properties of the HTL without and with ionic liquid were analyzed using the AFM technique. The effect of ionic-liquid incorporation on the device's performance was also investigated by measuring the active layer's surface morphology and device's efficiency.

2. Materials and Methods

2.1. Materials

PTB7 (poly({4,8-bis[(2-ethylhexyl)oxy]benzo [1,2-b:4,5-b']dithiophene-2,6-diyl} {3-fluoro-2-[(2-ethylhexyl)carbonyl]thieno[3,4-b]thiophenediyl}), average Mw 80,000–200,000), PCBM ([6,6]-phenyl C71 butyric acid methyl ester, 99%), ionic liquid BMIM+Cl-, acidic PEDOT:PSS (Aldrich No. 739332), pH-neutral PEDOT:PSS (Aldrich No. 739324), PEO (polyethylene oxide), n-propanol, chlorobenzene (CB), and other chemicals were purchased from Aldrich (Burlington, MA, USA) and used as received. The active layers of OSC devices were prepared using PTB7 and PCBM as the organic electron donor and electron acceptor material, respectively. Figure 1 shows the molecular structure of PTB7, PCBM, and BMIM+Cl-.

Energies **2023**, 16, 467 3 of 11

Figure 1. Molecular structure of PTB7, PCBM, and BMIM⁺Cl⁻.

2.2. Device Fabrication

Modified acidic and pH-neutral PEDOT:PSS solutions were prepared as follows: ionic liquid BMIM+Cl was dissolved in DI water at concentration of 100 mg/mL, and after that certain volume of BMIM+Cl/DI water was added to 1ml acidic or neutral PEDOT:PSS solution to obtain a 0.75, 0.5, 0.3, and 0.15 wt% BMIM+Cl-modified PEDOT:PSS solution. Solar cells with structure of glass/ITO/PEDOT:PSS/PTB7:PCBM/PEO/EGaIn were fabricated using a solution process. First, patterned indium tin oxide (ITO)-coated glass substrates with a sheet resistance of 7.5 Ω /square were cleaned with detergent, consequently being ultra-sonicated in isopropyl alcohol, methanol, and acetone for 15 min each. Solution of BMIM+Cl--modified PEDOT:PSS was spin-coated on top of the ITO surface to form a buffer layer (40–60 nm), before drying the substrates at 120 °C in an oven for 20 min. PTB7:PCBM blend solution was prepared by dissolve PTB7, PCBM (weight ratio 1:1.5), and 1,8-octanedithiol additive (2.5% vol) in chlorobenzene. The blend solution was ultrasonicated for 2 h and then stirred at 50 °C for more than 24 h before spin casting at 1500 rpm for 60 s to form the blending layer. Thickness of active layer was about 90–100 nm, as confirm by a profilometer. The samples were dried for 2 h at room temperature in glove box before the deposition of a PEO interfacial layer from a mixed solvent of 1 mg polyethylene oxide in 10 mL H₂O/n-propanol (50:50, vol/vol). After the deposition of PEO layer, samples were transferred to a hot plate and dried at 140 °C for 5 min. Finally, the EGaIn cathode was deposited on top of the PEO layer by doctor blading through a customized mask [25]. The active area of the device was 0.09 cm². The structure of the OSC devices is shown in Figure 2.

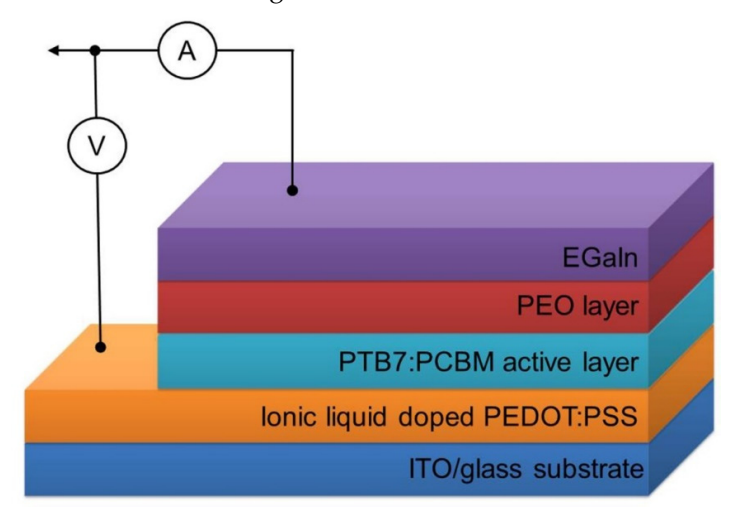


Figure 2. Cross-section view of PTB7:PCBM organic solar cells with ionic-liquid-doped PEDOT:PSS as the hole-transport layer and liquid EGaIn anode. Device structure of ITO/pHN-PEDOT:PSS/PTB7:PCBM/PEO/EGaIn was fabricated.

Energies 2023, 16, 467 4 of 11

2.3. Characterization

Transmittance spectra of PEDOT:PSS films were recorded over 200–1800 nm using a UV–vis spectrophotometer (Cary 5000, Varian, Palo Alto, CA, USA). The surface roughness and morphology images were characterized using atomic force microscope (AFM; NanoScope®IIIa, Digital Instruments, Veeco Metrology Group, Plainview, NY, USA) equipped with an extender module box operating in tapping mode under ambient condition. Current density–voltage (J–V) characteristics of PSC devices were measured using a Keithley 2400 source meter under simulated AM 1.5G radiation (100 mW/cm²). The power conversion efficiency (PCE) was calculated from the J–V characteristics. The conductivity of the films was determined by the four-point probe technique. The thickness of the PEDOT: PSS films was estimated with an Alpha D-120 stylus profilometer (KLA, Tencor, Milpitas, CA, USA). The devices were tested in the air without encapsulation, and all the measurements were performed at room temperature.

3. Results and Discussion

3.1. Effects of IL on the Optical Property of PEDOT:PSS Films

Figure 3a,b show the transmittance spectra of a BMIM $^+$ Cl $^-$ -doped acidic PEDOT:PSS film and a pH-neutral PEDOT:PSS film. The maximum transmittance of both the pristine acidic and pH-neutral PEDOT:PSS films was in the range of 96–97% within the wavelength range of 400–600 nm. The PEDOT:PSS films with ionic liquid B BMIM $^+$ Cl $^-$ exhibited slightly lower transmittance as compared to pristine PEDOT:PSS films. Doped PEDOT:PSS films at 0.75 wt% show a big difference compared to the others because, at a doping concentration of more than 0.5 wt%, the dispersion becomes viscous and is difficult to spin coat. At 550 nm, the transmittance of 0.75 wt% BMIM $^+$ Cl $^-$ -doped acidic PEDOT:PSS films decreases from 97.7% to 95.5%, while the transmittance of 0.75 wt% BMIM $^+$ Cl $^-$ -doped neutral PEDOT:PSS films decreases from 97.5% to 93.8%. It is important to note that at BMIM $^+$ Cl $^-$ -doping concentrations of lower than 0.5 wt%, the transmittance value still remains higher than 95%, which satisfies the minimum optical requirements for transparent electrodes (T > 90%) [17].

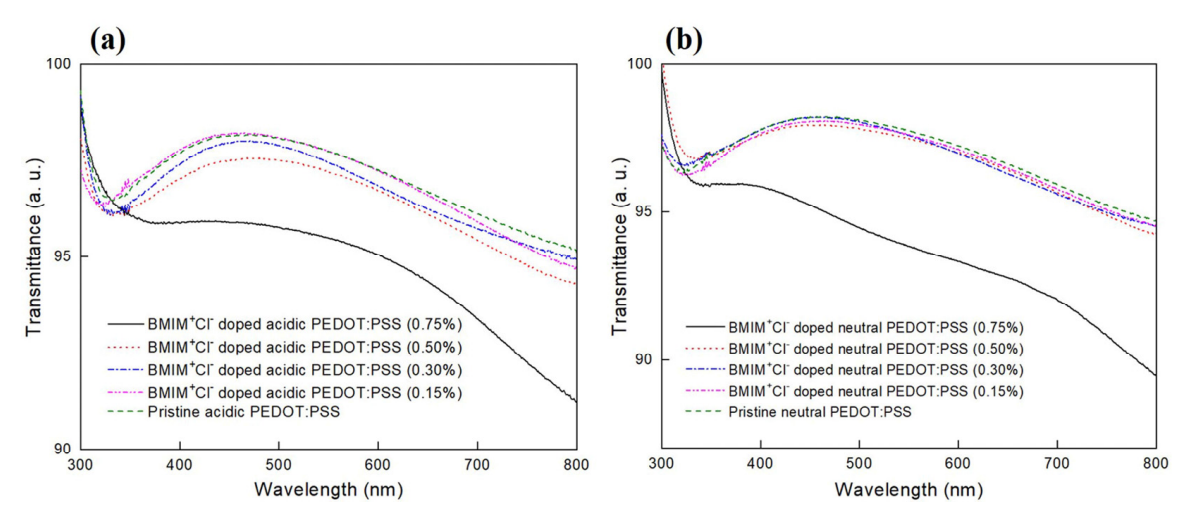


Figure 3. The transmittance spectra of BMIM⁺Cl⁻-doped (a) acidic PEDOT:PSS and (b) pH-neutral PEDOT:PSS films at different concentrations.

3.2. Effects of IL on the Conductivity and Morphology Properties of PEDOT:PSS Films

For each type of sample, four films were prepared. Conductivity was measured using the four-point probe technique at 10 different locations on each film, and an average of the measured values was taken. The results are presented in Table 1. A comparison of the conductivity values between the two pristine dispersions shows that the films based on the acidic PEDOT:PSS dispersion have about 2.5–3.0 higher conductivity than the films based on pH-neutral PEDOT:PSS dispersion. The reversed trends on how the ionic liquid

Energies 2023, 16, 467 5 of 11

affects the conductivity when doping BMIM $^+$ Cl $^-$ to acidic and pH-neutral PEDOT:PSS dispersions was observed. In the case of BMIM $^+$ Cl $^-$ -doped acidic PEDOT:PSS, the sheet resistance was increased slightly, consequently reducing the conductivity; when the doping concentration increased from 0 to 0.5 wt%, the sheet resistance increased from 242.3 k Ω /sq to 352.2 k Ω /sq, and the conductivity decreased from 1.03 to 0.47 S/cm, respectively. In the case of BMIM $^+$ Cl $^-$ -doped pH-neutral PEDOT:PSS films, however, the sheet resistance decreased dramatically; when the doping concentration increased from 0 to 0.5 wt%, the sheet resistance decreased from 759.7 k Ω /sq to 7.6 k Ω /sq, leading to an increasing of conductivity from 0.31 to 21.66 S/cm, which is an increase by a factor of 70 compared to pristine neutral PEDOT:PSS films. These trends are illustrated in Table 1 and Figure 4.

Table 1. Sheet resistance, film thickness, and conductivity of BMIM⁺Cl⁻-doped (a) acidic PEDOT:PSS and (b) neutral PEDOT:PSS films prepared on glass substrates at spin speed of 4000 rpm in 60 s.

	(a) Acidic	PEDOT:PSS, 1.1 wt%	$_{0}$, pH < 2.5		
Concentration of BMIM+Cl-(wt%)	Sheet Resistance (kΩ/sq)	Film Thickness (nm)	Resistivity (Ω·cm)	Conductivity (S/cm)	pН
0.00	242.3	40	0.969	1.03	2.3
0.15	278.4	45	1.25	0.80	2.8
0.30	303.2	50	1.52	0.66	3.2
0.50	352.2	60	2.11	0.47	3.6
	(b) pH-Neuti	al PEDOT:PSS, 1.1 w	rt%, pH = 5–7		
Concentration of BMIM ⁺ Cl ⁻ (wt%)	Sheet Resistance (kΩ/sq)	Film Thickness (nm)	Resistivity (Ω·cm)	Conductivity (S/cm)	pН
0.00	795.7	40	3.18	0.31	5.8
0.15	71.4	45	0.321	3.11	6.0
0.30	18.1	50	0.09	11.10	6.5
0.50	7.6	60	0.0462	21.66	6.8

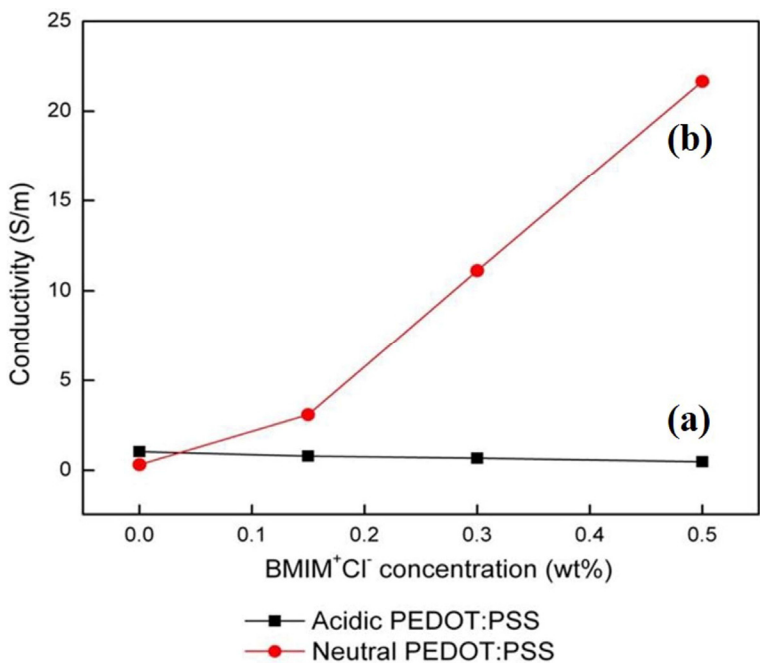


Figure 4. The conductivity of BMIM⁺Cl⁻-doped (**a**) acidic PEDOT:PSS and (**b**) pH-neutral PEDOT:PSS films.

Energies 2023, 16, 467 6 of 11

The reversed changing trends for conductivity can be explained based on the change of pH of the PEDOT:PSS dispersion when doping with BMIM $^+$ Cl $^-$. The chemical structure of PEDOT:PSS is shown in Figure 5a, in which positively charged conjugated PEDOT was neutralized by a negatively charged saturated PSS agent. The shorter PEDOT chain will be attached to the longer PSS chain by a weak dipole interaction between the SO $_3$ $^-$ group and thiophene ring [17]. Alternation of the pH will lead to a change in the way that the PSS chains interact with the PEDOT chains, leading to different distributions of the PEDOT grains and PSS grains on the surface of the PEDOT:PSS thin film.

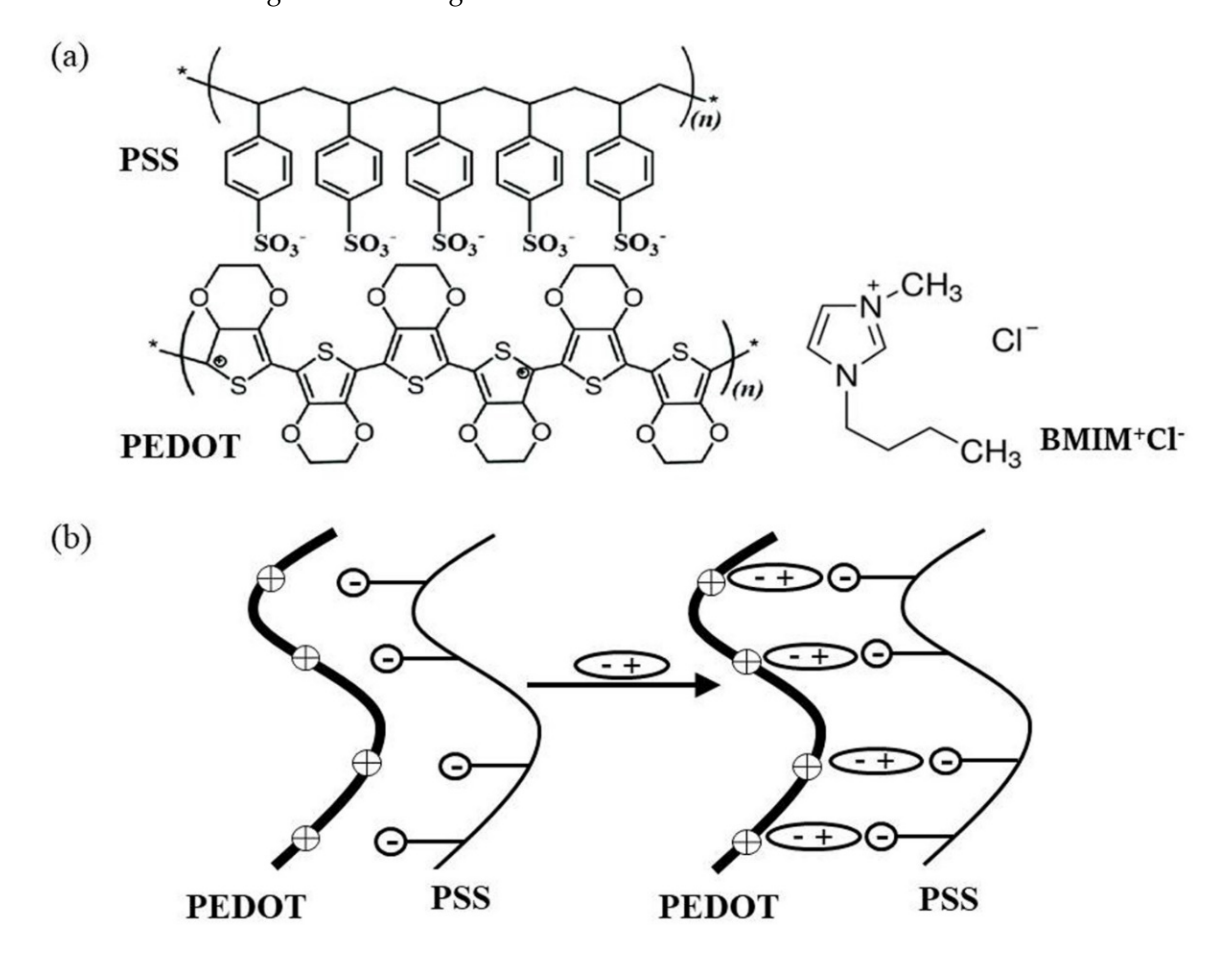


Figure 5. (a) Binding effect and (b) pushing effect when doping BMIM⁺Cl⁻ into PEDOT:PSS dispersion.

Naturally, ionic liquid BMIM⁺Cl⁻ is a weak base [26,27]; therefore, the addition of BMIM⁺Cl⁻ to an acidic PEDOT:PSS solution will increase the concentration of the -SO₃⁻ group (a pH change from 2 to 3–4, as confirmed by a pH indicator), resulting in an enhancement of the ability of the PEDOT chain attached to the PSS chain (Figure 5a). Our hypothesis was confirmed by the AFM results shown in Figure 6a: when the doping concentrations of BMIM⁺Cl⁻ increased from 0 to 0.5 wt%, the RMS value of the surface of a BMIM⁺Cl⁻-doped acidic PEDOT:PSS thin film decreased slightly from 1.062 to 0.944 nm. The smoother AFM surface indicated better mixing between the PEDOT chains and PSS chains, which raises the sheet resistance of the thin film and reduces the conductivity.

It should be noted that the chloride ion pairs in BMIM⁺Cl⁻ also have the ability to separate PEDOT chains from PSS chains (the so-called "pushing effect"), as shown in Figure 5b [28]. However, this effect is smaller than the "binding effect", in the case of BMIM⁺Cl⁻-doped acidic PEDOT:PSS.

Energies 2023, 16, 467 7 of 11

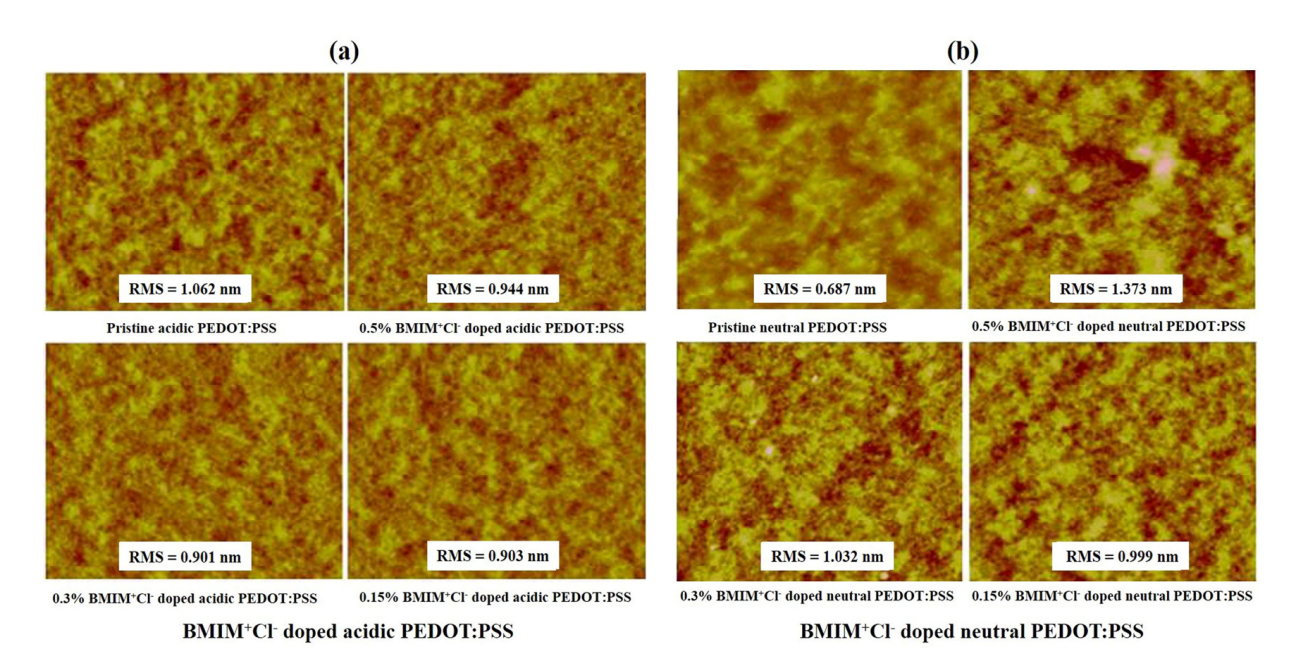


Figure 6. Surface morphology characterization, tapping mode AFM images of BMIM $^+$ Cl $^-$ -doped (a) acidic PEDOT:PSS and (b) neutral PEDOT:PSS at different concentrations of ionic liquid (the size of the scanned area was 2 \times 2 μ m).

In the case of BMIM⁺Cl⁻-doped neutral PEDOT:PSS, the pH of the neutral PEDOT:PSS dispersion does not change much when the concentrations of BMIM⁺Cl⁻ increased, so the "pushing" effect is the dominant effect compared with the "binding" effect. As illustrated in Figure 5b, BMIM⁺Cl⁻ ion pairs were inserted between the PEDOT chain and the PSS chain, pushing the PEDOT chain away from the PSS chain, resulting in the phase separation of the PEDOT and PSS chains, which makes the surface of PEDOT:PSS films rougher and, therefore, increases the conductivity [22–24]. Figure 6b is the AFM images of BMIM+Cl-doped neutral PEDOT:PSS; when increasing the concentration of BMIMCl doping, the RMS value of the thin film increases. Note that at the highest doping concentration, the RMS value of the film is 1.373 nm, which is nearly double the RMS value of pristine neutral PEDOT:PSS films; however, these RMS values are still good enough for organic solar cell application. When the BMIM+Cl⁻ is doped into the PEDOT:PSS, pushing the PEDOT chain away from the PSS chain leads to an increase in surface roughness. This increase in surface roughness corresponds to the phase separation between the PEDOT chains and PSS chains, leads to a reduction in the sheet resistance, an increase in the conductivity, and an improvement in the adhesion of the active layer to the PEDOT:PSS layer.

To conclude, the most significant increase in conductivity is induced by the addition of the ionic liquid BMIM⁺Cl⁻ into the pH-neutral PEDOT:PSS solution, while the addition of BMIM⁺Cl⁻ into the acidic PEDOT:PSS solution gives a negative effect.

3.3. Effects of IL Doping on the Electrical Property of the VFPH Solar Cells

The photovoltaic properties of PEDOT:PSS/PTB7:PCBM/PEO/EGaIn VFPH SCs using acidic or neutral PEDOT:PSS layers doped by ionic liquid BMIM $^+$ Cl $^-$ were investigated. Figures 7 and 8 shows the J–V curves of the VFPH SCs device with- BMIM $^+$ Cl $^-$ -doped acidic PEDOT:PSS and with- BMIM $^+$ Cl $^-$ -doped neutral PEDOT:PSS. The photovoltaic parameters (V $_{oc}$, J $_{sc}$, fill factor, and PCE) of the devices are listed in Table 2. Devices with a pristine acidic PEDOT:PSS layer exhibited PV performance with V $_{oc}$ = 0.71 V, J $_{sc}$ = 14.8 mA/cm 2 , FF = 38.8%, and PCE = 4.0%. Our V $_{oc}$ results were similar with those reported for PTB7:PCBM OPV devices, but the fill factor and J $_{sc}$ are much lower. One possible reason for the low FF and J $_{sc}$ is that the deposition step of the PEO layer from a mixed solvent of alcohol + water and an EGaIn electrode was completed outside the glove box. This step can cause a high probability of oxygen traps to appear in the PTB7:PCBM

Energies 2023, 16, 467 8 of 11

active layer and cause the formation of a space-charge-limited current (SCLC); as a result, the fill factor and J_{sc} were reduced compared with the reported devices. Devices with ionic liquid BMIM $^+$ Cl $^-$ -doped acidic PEDOT:PSS layers have demonstrated a slight decrease in PV performance, as revealed in Figure 7, and the results are summarized in Table 2. We concluded that the decrease in the conductivity and increase in the smoothness of the PEDOT:PSS film due to the addition of ionic liquid BMIM $^+$ Cl $^-$ in the acidic PEDOT:PSS dispersion has a deleterious effect on the performance of VFPH solar cells.

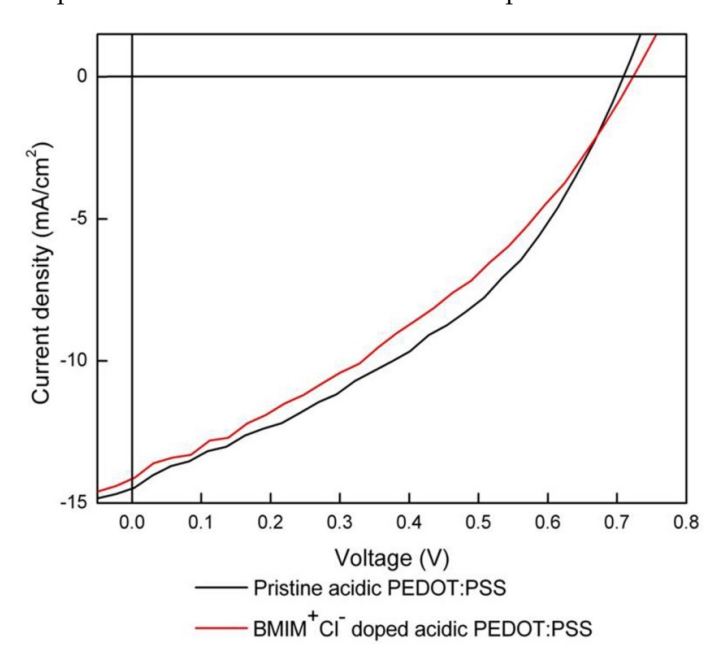


Figure 7. Current density–voltage (J–V) characteristics of PTB7:PCBM solar cells with pristine acidic PEDOT:PSS and BMIM⁺Cl⁻-doped acidic PEDOT:PSS as hole-transport layer (used with liquid EGaIn cathode).

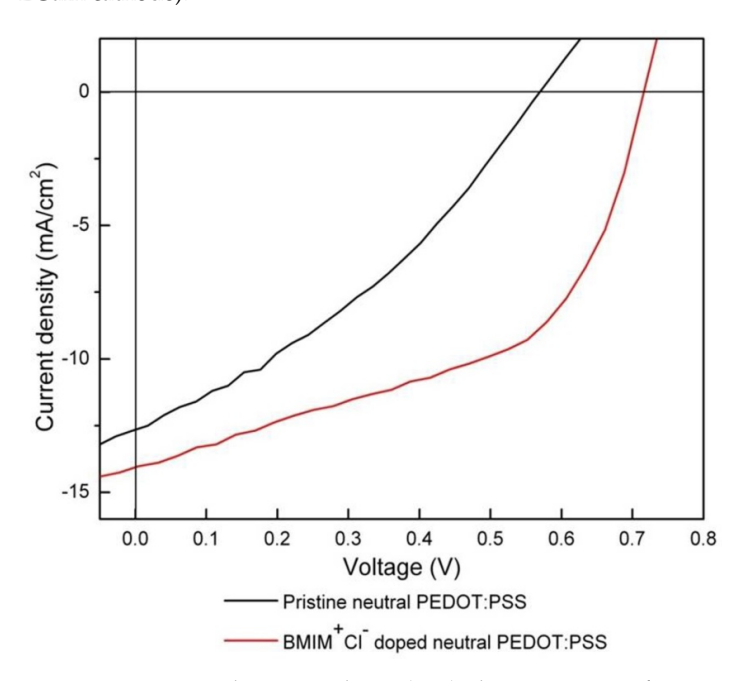


Figure 8. Current density–voltage (J–V) characteristics of PTB7:PCBM solar cells used with liquid EGaIn cathode and with pristine and BMIM⁺Cl⁻-doped neutral PEDOT:PSS as the hole-transport layer.

Energies 2023, 16, 467 9 of 11

PTB7:PCBM Solar Cells with EGaIn Electrode	V _{oc} (V)	J _{sc} (mA/cm ²)	FF (%)	PCE (η) (%)	Rs (Ω)
Pristine acidic PEDOT:PSS	0.71 ± 0.01 (0.71)	14.8 ± 0.2 (14.8)	38.8 ± 0.2 (39.1)	4.0 ± 0.2 (4.0)	455 ± 8 (462)
MIM ⁺ Cl ⁻ -doped acidic PEDOT:PSS	0.72 ± 0.00 (0.72)	14.1 ± 0.1 (14.1)	34.7 ± 0.1 (34.8)	3.5 ± 0.2 (3.5)	622 ± 5 (628)

Table 2. Photovoltaic parameters of PTB7:PCBM solar cells with BMIM⁺Cl⁻-doped acidic PEDOT:PSS as hole-transport layers used with liquid EGaIn electrode.

Table 3 lists the corresponding cell parameters J_{sc} , V_{oc} , and FF and the resistance of PSC devices in the case of ionic liquid BMIM⁺Cl⁻-doped pH-neutral PEDOT:PSS dispersion. It can be observed that the utilization of a BMIM⁺Cl⁻-doped pH-neutral PEDOT:PSS dispersion leads to a simultaneous improvement of J_{sc} , V_{oc} , and FF, corresponding to a higher efficiency of VFPH SCs devices. Devices with a pH-neutral PEDOT:PSS hole-transport layer only achieve 2.8% efficiency, whereas solar cell devices using a BMIM⁺Cl⁻-doped pH-neutral PEDOT:PSS as the hole-transport layer improve up to ~5.0%. The improvement of the final device performance when using a BMIM⁺Cl⁻-doped pH-neutral PEDOT:PSS is mainly ascribed to the increase in conductivity, which helps reduce the sheet resistance and leads to the simultaneous improvement of J_{sc} , V_{oc} and FF. When the conductivity increases from 0.31 S/cm to 21 S/cm, the sheet resistance reduces from 862 Ω to 90 Ω , which leads to a significant increase in V_{oc} , from 0.60 V to 0.72 V; an increase in J_{sc} , from 12.8 mA/cm² to 14.3 mA/cm²; and also a decent enhancement of FF from 34.3% to 47.7%.

Table 3. Photovoltaic parameters of PTB7:PCBM solar cells with BMIM⁺Cl⁻-doped neutral PE-DOT:PSS as hole-transport layers used with liquid EGaIn electrode.

PTB7:PCBM Solar Cells with EGaIn Electrode	V _{oc} (V)	J _{sc} (mA/cm ²)	FF (%)	PCE (η) (%)	Rs (Ω)
pristine neutral PEDOT:PSS	0.60 ± 0.01 (0.60)	12.7 ± 0.2 (12.8)	34.0 ± 0.2 (34.3)	2.6 ± 0.1 (2.8)	853 ± 7 (862)
BMIM ⁺ Cl ⁻ -doped neutral PEDOT:PSS	0.72 ± 0.00 (0.72)	14.0 ± 0.3 (14.3)	47.7 ± 0.2 (47.9)	4.8 ± 0.2 (5.0)	85 ± 3 (90)

Compared with a vacuum-process—organic hybrid solar cell with a recorded efficiency of about ~12%, the efficiency of this study is still low. However, we have reported a new vacuum-free structure, which has a simple and inexpensive fabrication process. The device's performance might be enhanced by optimizing the device's nanostructure and light-absorption percentage and the charge carrier's collection.

4. Conclusions

The effects of doping ionic liquid BMIM+Cl⁻ on the conductivity and surface morphology of acid and pH-neutral PEDOT:PSS films were investigated. The conductivity of the acid and pH-neutral PEDOT:PSS films could be tuned through a treatment with BMIM+Cl⁻ ionic liquid. In the case of the acidic PEDOT:PSS, the conductivity decreased because the ionic liquid can enhance the ability of the PEDOT chains to stick to the PSS chains. In the case of the pH-neutral PEDOT:PSS, the ion pair of the ionic liquid effectively reduces the coulombic attraction between the PEDOT and PSS chains, resulting in a good separation of the PSS chains from the PEDOT chains, which, therefore, increases the conductivity and leads to better performance by the OSC devices. The surface morphology of the acid and pH-neutral PEDOT:PSS films were slightly increased due to pushing the PEDOT chain away from the PSS chain. Maximum power conversion efficiency (~5.0%) was achieved on PTB7:PCBM PSCs with ionic liquid BMIM+Cl⁻-treated pH-neutral PEDOT:PSS films as the anode and liquid EGaIn as the cathode. Furthermore, the device's efficiency can

Energies **2023**, 16, 467 10 of 11

be improved by optimizing the active layer's morphology and light absorption, by the incorporation of metal plasmonic. This result will be reported soon in our future work.

Author Contributions: Conceptualization, V.T.H.P. and T.K.T.; Writing—original draft preparation, V.T.H.P. and T.K.T.; data interpretation, V.T.H.P., T.K.T., H.M.S. and A.A.; data curation, V.T.H.P., H.M.S. and N.T.N.T.; funding acquisition, H.M.S. and S.M.A.-Z.; validation, V.T.H.P., T.K.T., A.A. and S.B.D.; resources, T.K.T. and H.M.S.; writing—review and editing, M.S.T.; supervision, project administration, N.T.N.T. All authors have read and agreed to the published version of the manuscript.

Funding: This research was funded by Deputyship for Research and Innovation, Ministry of Education, Saudi Arabia, through project no.(IFKSURG-2-1372).

Institutional Review Board Statement: Not applicable.

Informed Consent Statement: Not applicable.

Data Availability Statement: Not applicable.

Acknowledgments: The authors extend their appreciation to the Deputyship for Research and Innovation, Ministry of Education, Saudi Arabia, for funding this research work through project no. (IFKSURG-2-1372).

Conflicts of Interest: The authors declare that they have no known competing financial interest or personal relationships that could appear to influence the work reported in this paper.

References

- 1. Fu, H.; Li, Y.; Yu, J.; Wu, Z.; Fan, Q.; Lin, F.; Woo, H.Y.; Gao, F.; Zhu, Z.; Jen, A.K.Y. High efficiency (15.8%) all-polymer solar cells enabled by a regioregular narrow bandgap polymer acceptor. *J. Am. Chem. Soc.* **2021**, 143, 2665–2670. [CrossRef] [PubMed]
- 2. Park, M.; Jung, J.W. Easily Accessible Low Band Gap Polymer for Efficient Nonfullerene Polymer Solar Cells with a Low Eloss of 0.55 eV. ACS Appl. Mater. Interfaces 2019, 11, 5435–5440. [CrossRef] [PubMed]
- 3. Scharber, M.C.; Sariciftci, N.S. Efficiency of bulk-heterojunction organic solar cells. *Prog. Polym. Sci.* **2013**, *38*, 1929–1940. [CrossRef] [PubMed]
- 4. Liu, C.; Yi, C.; Wang, K.; Yang, Y.; Bhatta, R.S.; Tsige, M.; Xiao, S.; Gong, X. Single-junction polymer solar cells with over 10% efficiency by a novel two-dimensional donor–acceptor conjugated copolymer. *ACS Appl. Mater. Interfaces* **2015**, *7*, 4928–4935. [CrossRef]
- 5. Hou, J.; Inganas, O.; Friend, R.H.; Gao, F. Organic solar cells based on non-fullerene acceptors. *Nat. Mater.* **2018**, *17*, 119–128. [CrossRef]
- 6. Cheng, P.; Li, G.; Zhan, X.; Yang, Y. Next-generation organic photovoltaics based on non-fullerene acceptors. *Nat. Photonics.* **2018**, 12, 131–142. [CrossRef]
- 7. Weng, K.; Ye, L.; Zhu, L.; Xu, J.; Zhou, J.; Feng, X.; Lu, G.; Tan, S.; Liu, F.; Sun, Y. Optimized active layer morphology toward efficient and polymer batch insensitive organic solar cells. *Nat. Commun.* **2020**, *11*, 2855. [CrossRef]
- 8. Ayzner, A.L.; Wanger, D.D.; Tassone, C.J.; Tolbert, S.H.; Schwartz, B.J. Room to Improve Conjugated Polymer-Based Solar Cells: Understanding How Thermal Annealing Affects the Fullerene Component of a Bulk Heterojunction Photovoltaic Device. *J. Phys. Chem. C* 2008, 112, 18711–18716. [CrossRef]
- 9. Verploegen, E.; Mondal, R.; Bettinger, C.J.; Sok, S.; Toney, M.F.; Bao, Z. Effects of thermal annealing upon the morphology of polymer–fullerene blends. *Adv. Funct. Mater.* **2010**, *20*, 3519–3529. [CrossRef]
- 10. Li, G.; Yao, Y.; Yang, H.; Shrotriya, V.; Yang, G.; Yang, Y. "Solvent annealing" effect in polymer solar cells based on poly (3-hexylthiophene) and methanol fullerenes. *Adv. Funct. Mater.* **2007**, 17, 1636–1644. [CrossRef]
- 11. Kumar, C.V.; Cabau, L.; Viterisi, A.; Biswas, S.; Sharma, G.D.; Palomares, E. Solvent annealing control of bulk heterojunction organic solar cells with 6.6% efficiency based on a benzodithiophene donor core and dicyano acceptor units. *J. Phys. Chem. C* **2015**, *119*, 20871–20879. [CrossRef]
- 12. Liao, H.C.; Ho, C.C.; Chang, C.Y.; Jao, M.H.; Darling, S.B.; Su, W.F. Additives for morphology control in high-efficiency organic solar cells. *Mater. Today* **2013**, *16*, 326–336. [CrossRef]
- 13. Schmidt, K.; Tassone, C.J.; Niskala, J.R.; Yiu, A.T.; Lee, O.P.; Weiss, T.M.; Wang, C.; Frechet, J.M.J.; Beaujuge, P.M.; Toney, M.F. A Mechanistic Understanding of Processing Additive-Induced Efficiency Enhancement in Bulk Heterojunction Organic Solar Cells. *Adv. Mater.* 2014, 26, 300–305. [CrossRef] [PubMed]
- 14. Lattante, S. Electron and hole transport layers: Their use in inverted bulk heterojunction polymer solar cells. *Electronics* **2014**, *3*, 132–164. [CrossRef]
- 15. Chen, L.M.; Xu, Z.; Hong, Z.; Yang, Y. Interface investigation and engineering—Achieving high performance polymer photovoltaic devices. *J. Mater. Chem.* **2010**, *20*, 2575–2598. [CrossRef]
- 16. Park, J.H.; Lee, T.W.; Chin, B.D.; Wang, D.H.; Park, O.O. Roles of interlayers in efficient organic photovoltaic devices. *Macromol. Rapid Commun.* **2010**, *31*, 2095–2108. [CrossRef]

Energies 2023, 16, 467 11 of 11

17. Sun, K.; Zhang, S.; Li, P.; Xia, Y.; Zhang, X.; Du, D.; Isikgor, F.H.; Ouyang, J. Review on application of PEDOTs and PEDOT: PSS in energy conversion and storage devices. *J. Mater. Sci. Mater. Electron.* **2015**, *26*, 4438–4462. [CrossRef]

- 18. Park, H.; Kong, J. An Alternative Hole Transport Layer for Both ITO-and Graphene-Based Organic Solar Cells. *Adv. Energy Mater.* **2014**, *4*, 1301280. [CrossRef]
- 19. Kim, J.Y.; Jung, J.H.; Lee, D.E.; Joo, J. Enhancement of electrical conductivity of poly (3, 4-ethylenedioxythiophene)/poly (4-styrenesulfonate) by a change of solvents. *Synth. Met.* **2002**, *126*, 311–316. [CrossRef]
- 20. Ouyang, J.; Xu, Q.; Chu, C.W.; Yang, Y.; Li, G.; Shinar, J. On the mechanism of conductivity enhancement in poly (3, 4-ethylenedioxythiophene): Poly (styrene sulfonate) film through solvent treatment. *Polymer* **2004**, *45*, 8443–8450. [CrossRef]
- 21. Jonsson, S.K.M.; Birgerson, J.; Crispin, X.; Greczynski, G.; Osikowicz, W.; Denier van der Gon, A.W.; Salaneck, W.R.; Fahlman, M. The effects of solvents on the morphology and sheet resistance in poly (3, 4-ethylenedioxythiophene)–polystyrenesulfonic acid (PEDOT–PSS) films. *Synth. Met.* **2003**, 139, 1–10. [CrossRef]
- 22. Xia, Y.; Zhang, H.; Ouyang, J. Highly conductive PEDOT: PSS films prepared through a treatment with zwitterions and their application in polymer photovoltaic cells. *J. Mater. Chem.* **2010**, *20*, 9740–9747. [CrossRef]
- 23. Kadem, B.; Cranton, W.; Hassan, A. Metal salt modified PEDOT: PSS as anode buffer layer and its effect on power conversion efficiency of organic solar cells. *Org. Electron.* **2015**, *24*, 73–79. [CrossRef]
- 24. Badre, C.; Marquant, L.; Alsayed, A.M.; Hough, L.A. Highly conductive poly (3, 4-ethylenedioxythiophene): Poly (styrene-sulfonate) films using 1-ethyl-3-methylimidazolium tetracyanoborate ionic liquid. *Adv. Funct. Mater.* **2012**, 22, 2723–2727. [CrossRef]
- 25. Pham, V.T.H.; Trinh, T.K.; Truong, N.T.N.; Park, C. Liquid eutectic GaIn as an alternative electrode for PTB7: PCBM organic solar cells. *Jpn. J. Appl. Phys.* **2017**, *56*, 046501. [CrossRef]
- 26. Cuilian, Y.; Lixia, H.; Hang, S.; Kaihua, G. Determination of pH value and acid-base Property of Ionic Liquid Aqueous Solutions. *Acta Chim. Sin.* **2014**, 72, 495–501.
- 27. Zhanying, Z.; Hara, I.M.O.; William, O.S.D. Effects of pH on pretreatment of sugarcane bagasse using aqueous imidazolium ionic liquids. *Green Chem.* **2013**, *15*, 431–438. [CrossRef]
- 28. Dobbelin, M.; Marcilla, R.; Salsamendi, M.; Gonzalo, C.P.; Carrasco, P.M.; Pomposo, J.A.; Mecerreyes, D. Influence of ionic liquids on the electrical conductivity and morphology of PEDOT: PSS films. *Chem. Mater.* **2007**, *19*, 2147–2149. [CrossRef]

Disclaimer/Publisher's Note: The statements, opinions and data contained in all publications are solely those of the individual author(s) and contributor(s) and not of MDPI and/or the editor(s). MDPI and/or the editor(s) disclaim responsibility for any injury to people or property resulting from any ideas, methods, instructions or products referred to in the content.